Estrada-Jimenez, J. C., Guzman, B. G., Fernandez-Getino Garcia, M. J. & Jimenez, V. P. G. (2019). Superimposed Training-Based Channel Estimation for MISO Optical-OFDM VLC. *IEEE Transactions on Vehicular Technology*, 68(6), pp. 6161–6166.

DOI: 10.1109/tvt.2019.2909428

Superimposed Training-based Channel Estimation for MISO Optical-OFDM VLC

Juan Carlos Estrada-Jiménez, *Student Member, IEEE,* Borja Genovés Guzmán, *Student Member, IEEE,* M. Julia Fernández-Getino García, *Member, IEEE,* Víctor P. Gil Jiménez, *Senior Member, IEEE.*

***Abstract*—In this paper we investigate a novel channel estimation method for multiple-input and single-output (MISO) systems in visible light communication (VLC). Direct current biased optical orthogonal frequency division multiplexing (DCO-OFDM) is commonly used in VLC where half of the available subcarriers are spent to guarantee a real-valued output after the inverse fast Fourier transform operation. Besides, dedicated subcarriers are typically used for channel estimation (CE), thus, many resources are wasted and the spectral efficiency is degraded. We propose a superimposed training approach for CE in MISO DCO-OFDM VLC scenarios. Analytical expressions of mean squared error (MSE) and spectral efficiency are derived when the least squares estimator is considered. This analysis is valid for outdoor and indoor scenarios. For the channel estimation error, simulation results of MSE show a perfect match with analytical expressions. Moreover, results prove that this technique guarantees a larger spectral efficiency than previous schemes where dedicated pilots were used. Finally, the optimal data power allocation factor is also analytically derived.**

***Index Terms*—Channel estimation, DCO-OFDM, superimposed training, visible light communication.**

I. Introduction

Visible light communication (VLC) is a promising technology to satisfy the growing demand for higher data rates in wireless communications. It is expected that VLC can meet the new demands for spectral efficiency that cannot be achieved by radio frequency (RF) technologies. Moreover, VLC and RF technologies can work together creating a hybrid network [1]. This technology allows us to provide illumination and convey information through a light-emitting diode (LED), while the information is received and converted from optical to electrical signal by a photodiode (PD). Several multicarrier modulation techniques have been developed in optics [2], such as direct current biased optical orthogonal frequency division multiplexing (DCO-OFDM), asymmetrically clipped optical OFDM (ACO-OFDM) or unipolar OFDM (U-OFDM).

Multiple-input and multiple-output (MIMO) techniques have been extensively considered in RF. However, in VLC MIMO channels are not as decorrelated as in RF and the multiplexing gain is not easily achieved. Thus, full rank channel matrices must be obtained through the construction of larger receiver arrays [3]. In an indoor scenario multiple LEDs are required to accomplish both the illumination requirements and to transmit information. Therefore, multiple-input and single-output (MISO) techniques are more suitable to be considered in real indoor VLC scenarios [4] [5]. Indeed, they have been mentioned in the literature as interesting techniques to exploit the spatial multiplexing and diversity [6]. In these MISO schemes, the channel state information can be used at the receiver for equalization, or at the transmitter for precoding purposes. To that end, in several papers the authors assume perfect knowledge of the channel [7], which could be valid if the user is fairly static but it is not always the case. Several channel estimation techniques have been proposed for VLC using dedicated pilot schemes in MISO scenarios [8] in quasi-stationary environments where the channel changes after a determined number of OFDM symbols. In [9], a Bayesian channel estimator is proposed for VLC using pilot symbol assisted modulation (PSAM) techniques. However, PSAM reduces the spectral efficiency considerably because several subcarriers need to be dedicated to pilots transmission. By contrast, superimposed training (ST) is a channel estimation technique, already proposed in RF systems [10] [11], where the pilot signal is arithmetically added to the data signal using the same resources without wasting dedicated subcarriers. A first approach to ST applied to a VLC scenario with single-LED transmission was proposed in [12]. However, to the best of our knowledge, no research on ST-based channel estimation in MISO-VLC scenarios has been developed.

Against this background, we propose a MISO-VLC system with ST avoiding the use of dedicated resources for channel estimation purposes. Superimposed training cannot be straightforwardly used on VLC, and thus, an analysis of the effective combination of both techniques with parameters adapted to the new MISO-VLC conditions must be carried out. Analytical expressions of mean squared error (MSE) with the least squares (LS) estimator are theoretically derived and they perfectly match with simulation results. In addition, spectral efficiency expressions are obtained for MISO-VLC to prove that ST outperforms previous PSAM schemes in terms of spectral efficiency. Moreover, the optimal data power allocation factor is theoretically found and it fits simulation results.

The rest of this paper is organized as follows. Section II describes the system model for the proposed scheme. Section III presents the channel estimation scheme and the analytical expressions of the estimation error. Section IV provides the analysis of the spectral efficiency. Section V discusses the simulation and analytical results and finally Section VI presents the conclusions of the paper.

II. System Model for the Proposed Scheme

Let us consider a MISO DCO-OFDM system with N subcarriers and N_{t} transmission LEDs. DCO-OFDM is one of

This work has been partially funded by the National Secretary of Higher Education, Science, Technology and Innovation (SENESCYT) in Ecuador, the Spanish MECD FPU fellowship program granted to the author B. Genovés Guzmán and by the Spanish National Project TERESA-ADA (TEC2017-90093-C3-2-R) (MINECO/AEI/FEDER, UE). The authors are with the Department of Signal Theory and Communications of the University Carlos III of Madrid, Spain. Email: {jestrada, bgenoves, mjulia, vgil}@tsc.uc3m.es.

the most commonly used schemes for VLC due to its spectral efficiency and flexibility. Thus, we will consider it to illustrate our proposal, although this study can be easily extended to other optical OFDM-based schemes, such as ACO-OFDM.

To accomplish the illumination requirements and transmit information, MISO techniques are more suitable to be considered in real indoor VLC scenarios. This analysis is also valid for single-input and single-output (SISO) schemes where N_{t}=1. The frequency-domain transmitted signal, denoted by the $(N-2)\times 1$ vector $\mathbf{x}$, is composed of data and pilot symbols where $\mathbf{x}=\mathbf{d}+\mathbf{p}$, being $\mathbf{d}$ and $\mathbf{p}$ the frequency-domain data and pilot signals, respectively, which are $(N-2)\times 1$ vectors with values $d(k)$ and $p(k)$. The subcarrier's index k takes values in the set $\{1,...,N/2-1\}\cup\{N/2+1,...,N-1\}$, because a DCO-OFDM modulation technique is used. Thus, the symbols conveyed on the subcarriers with indices $\{N/2+1,...,N-1\}$ are Hermitian symmetric of the symbols carried on the subcarriers with indices $\{1,...,N/2-1\}$. That is, only half of the subcarriers carry useful information. In addition, 0-th and $N/2$-th subcarriers do not convey information. This arrangement guarantees a real-valued signal at the output of the inverse fast Fourier transform. We can describe the DCO-OFDM frequency-domain symbol as

$$\mathbf{x}=\begin{bmatrix}0 & \mathbf{x}_{\mathrm{C}}^{\mathrm{T}}[1,...,N/2-1] & 0 & \mathbf{x}_{\mathrm{C}}^{\mathrm{T}}[N/2,...,N-2]\end{bmatrix}^{\mathrm{T}} \quad (1)$$

where $\mathbf{x}_{\mathrm{C}}$ is an $(N/2-1)$-column vector and $\mathbf{x}_{\mathrm{C}}[N/2,...,N-2]=\left\{\mathbf{x}_{\mathrm{C}}^{\mathrm{T}}[1,...,N/2-1]\right\}^{\mathrm{H}}=\mathbf{x}_{\mathrm{half}}$. The transpose and the Hermitian transpose operators are denoted by $(\cdot)^{\mathrm{T}}$ and $(\cdot)^{\mathrm{H}}$, respectively. The DC-bias value expressed in the 0-th subcarrier is set to 0. It is used for locating the signal within the dynamic range of the LED. The dynamic range determines the clipping levels of the signal leading to clipping noise that follows a Gaussian distribution according to the Bussgang and the central limit theorems [13]. Since an additive white Gaussian noise (AWGN) will be considered in this work, the study of these parameters can be omitted [14]. VLC systems also suffer from shot and thermal noise, typically modeled as an AWGN [15], too. Thus, the power of these noise sources are usually denoted by a variance of their combination [8] [9] and it indirectly represents different user's locations in the scenario.

The total electrical transmit power is represented by $\mathcal{P}=\mathcal{P}_{\mathrm{D}}+\mathcal{P}_{\mathrm{P}}$, where $\mathcal{P}_{\mathrm{D}}$ is the power assigned to data symbols and $\mathcal{P}_{\mathrm{P}}$ is the power dedicated to pilots, computed by $\mathcal{P}_{\mathrm{D}}=\mathrm{E}\left[\mathbf{d}^{\mathrm{H}}\mathbf{d}\right]=\alpha\mathcal{P}$ and $\mathcal{P}_{\mathrm{P}}=\mathrm{E}\left[\mathbf{p}^{\mathrm{H}}\mathbf{p}\right]=(1-\alpha)\mathcal{P}$, respectively, where $\mathrm{E}[\cdot]$ represents the statistical expectation and α is the ratio between the power reserved for data symbols and the total power, usually denoted the data power allocation factor, and whose range is $0<\alpha<1$. The electrical power is assumed to be equally distributed among the $N-2$ subcarriers used for signal transmission. Thus, the transmitted power assigned to data and pilots in ST are $\mathrm{E}\left[|d_{\mathrm{ST}}(k)|^2\right]=\frac{\mathcal{P}_{\mathrm{D}}}{N-2}\quad\forall k, \mathrm{E}\left[|p_{\mathrm{ST}}(k)|^2\right]=\frac{\mathcal{P}_{\mathrm{P}}}{N-2}\quad\forall k$, and in PSAM are $\mathrm{E}\left[|d_{\mathrm{PSAM}}(k)|^2\right]=\frac{\mathcal{P}_{\mathrm{D}}}{N-N_{\mathrm{P}}-2}\quad k\in\mathcal{K}_{\mathrm{D}}$, $\mathrm{E}\left[|p_{\mathrm{PSAM}}(k)|^2\right]=\frac{\mathcal{P}_{\mathrm{P}}}{N_{\mathrm{P}}}\quad k\in\mathcal{K}_{\mathrm{P}}$, where $\mathcal{K}_{\mathrm{P}}$ and $\mathcal{K}_{\mathrm{D}}$ correspond to the disjoint sets of subcarriers dedicated to pilots and data symbols in PSAM, respectively, and N_{P} is the cardinality of pilot set $N_{\mathrm{P}}=|\mathcal{K}_{\mathrm{P}}|$. Note that, in ST, all the subcarriers conveying energy are simultaneously used for data symbols and pilots ($N_{\mathrm{P}}=N-2$). The received signal for SISO scenario can be represented by

$$y(k)=R_{\mathrm{pd}}H(k)x(k)+w(k), \quad (2)$$

where R_{pd} is the responsivity of the PD, $x(k)$ and $w(k)$ are the transmitted symbol and the AWGN in the k-th subcarrier, respectively, and $H(k)$ is the VLC channel gain in the k-th subcarrier from the transmitter to the PD. In a MISO case where N_{t} transmission LEDs are considered, the received signal is written as

$$y(k)=R_{\mathrm{pd}}\sum_{i=1}^{N_{\mathrm{t}}}H_i(k)x_i(k)+w(k), \quad (3)$$

where $x_i(k)$ and $H_{\mathrm{i}}(k)$ are the transmitted symbol by the i-th LED and the VLC channel gain from the i-th LED to the PD in the k-th subcarrier, respectively. The received signal can be written in vector form as

$$\mathbf{y}=R_{\mathrm{pd}}\sum_{i=1}^{N_{\mathrm{t}}}\mathbf{D}_i\mathbf{h}_{\mathrm{i}}^{\mathrm{f}}+\mathbf{w}, \quad (4)$$

where $\mathbf{y}$, $\mathbf{w}$ and $\mathbf{h}_{\mathrm{i}}^{\mathrm{f}}$ are $(N-2)\times 1$ vectors that represent the received symbols, the AWGN and the VLC channel gain from the i-th LED in frequency domain, respectively. Additionally, $\mathbf{D}_i=\mathrm{diag}\left(\mathbf{x}_{\mathrm{C}_i}\right)$ is an $(N-2)\times(N-2)$ diagonal matrix whose elements are $\mathbf{x}_{\mathrm{C}_i}$, which are the useful transmitted symbols by the i-th LED. The channel in frequency domain $\mathbf{h}_i^{\mathrm{f}}$ can be expressed as $\mathbf{F}\mathbf{h}_i$, where $\mathbf{F}$ is the $(N-2)\times L$ DFT matrix whose values are $[\mathbf{F}]_{k,l}=\mathbf{e}^{\frac{-j2\pi kl}{N}}$ being k and l the row and column indices, respectively. The i-th LED channel impulse response (CIR) is denoted by $\mathbf{h}_i$ and has a channel length of L. Taking into account that the symbol transmitted by the i-th LED is $\mathbf{x}_i=\mathbf{d}_i+\mathbf{p}_i$, the received symbols can be expressed as

$$\mathbf{y}=R_{\mathrm{pd}}\mathbf{D}_{\mathrm{DF}}\mathbf{h}+R_{\mathrm{pd}}\mathbf{D}_{\mathrm{PF}}\mathbf{h}+\mathbf{w}, \quad (5)$$

where $\mathbf{D}_{\mathrm{DF}}=[\mathbf{D}_{\mathrm{d}_1}\mathbf{F},\mathbf{D}_{\mathrm{d}_2}\mathbf{F},...,\mathbf{D}_{\mathrm{d}_{N_{\mathrm{t}}}}\mathbf{F}]$ and $\mathbf{D}_{\mathrm{PF}}=[\mathbf{D}_{\mathrm{p}_1}\mathbf{F},\mathbf{D}_{\mathrm{p}_2}\mathbf{F},...,\mathbf{D}_{\mathrm{p}_{N_{\mathrm{t}}}}\mathbf{F}]$, being $\mathbf{D}_{\mathrm{d}_i}$ and $\mathbf{D}_{\mathrm{p}_i}$ $(N-2)\times(N-2)$ diagonal matrices of $\mathbf{d}_i$ and $\mathbf{p}_i$, respectively. Since spatial diversity is performed, $\mathbf{d}_i=\mathbf{d}$. The complete channel in the time domain is represented by $\mathbf{h}=[\mathbf{h}_1^{\mathrm{T}},\mathbf{h}_2^{\mathrm{T}},...,\mathbf{h}_{N_{\mathrm{t}}}^{\mathrm{T}}]^{\mathrm{T}}$. Let us define $\mathbf{y}^{(\mathrm{P})}$ as the $N_{\mathrm{P}}\times 1$ vector containing the corresponding values at the pilot positions of $\mathbf{y}$. Assuming that the channel changes every M OFDM symbols, we can extract the pilot symbols as

$$\widetilde{\mathbf{y}}^{(\mathrm{P})}=R_{\mathrm{pd}}\mathbf{D}_{\mathrm{PF}}^{(\mathrm{P})}\mathbf{h}+\frac{1}{M}R_{\mathrm{pd}}\sum_{\mathrm{m}=1}^{M}\{\mathbf{D}_{\mathrm{DF}}^{(\mathrm{P})}\}_{\mathrm{m}}\mathbf{h}+\frac{1}{M}\sum_{\mathrm{m}=1}^{M}\mathbf{w}_{\mathrm{m}}^{(\mathrm{P})} \quad (6)$$

where $\widetilde{\mathbf{y}}^{(\mathrm{P})}$ is an $N_{\mathrm{P}}\times 1$ vector representing the M-averaged received signal at the corresponding pilot positions. $\mathbf{D}_{\mathrm{PF}}^{(\mathrm{P})}$, $\left\{\mathbf{D}_{\mathrm{DF}}^{(\mathrm{P})}\right\}_{\mathrm{m}}$ and $\mathbf{w}_{\mathrm{m}}^{(\mathrm{P})}$ are the corresponding $N_{\mathrm{P}}\times LN_{\mathrm{t}}$ matrices and $N_{\mathrm{P}}\times 1$ vector at the corresponding pilot positions and at the m-th OFDM symbol, where $m\in\{1,...,M\}$.

III. Channel Estimation

The LS channel estimator allows obtaining a simple and effective receiver. Besides, no additional parameters than the received signal and the knowledge of the pilot sequence are

required. A high performance is achieved with a reduced complexity.

A. LS channel estimation

The LS channel estimator [16] can be derived as

$$\hat{\mathbf{h}} = \frac{1}{R_{\mathrm{pd}}} \left(\left\{ \mathbf{D}_{\mathrm{PF}}^{(\mathrm{P})} \right\}^{\mathrm{H}} \mathbf{D}_{\mathrm{PF}}^{(\mathrm{P})} \right)^{-1} \left\{ \mathbf{D}_{\mathrm{PF}}^{(\mathrm{P})} \right\}^{\mathrm{H}} \widetilde{\mathbf{y}}^{(\mathrm{P})}. \quad (7)$$

Replacing (6) in (7), the channel estimation in the time domain can be written as

$$\begin{aligned} \hat{\mathbf{h}} = & \mathbf{h} + \frac{1}{M} \left(\left\{ \mathbf{D}_{\mathrm{PF}}^{(\mathrm{P})} \right\}^{\mathrm{H}} \mathbf{D}_{\mathrm{PF}}^{(\mathrm{P})} \right)^{-1} \left\{ \mathbf{D}_{\mathrm{PF}}^{(\mathrm{P})} \right\}^{\mathrm{H}} \\ & \cdot \left(\sum_{\mathrm{m}=1}^{M} \left\{ \mathbf{D}_{\mathrm{DF}}^{(\mathrm{P})} \right\}_{\mathrm{m}} \mathbf{h} + \frac{1}{R_{\mathrm{pd}}} \sum_{\mathrm{m}=1}^{M} \mathbf{w}_{\mathrm{m}}^{(\mathrm{P})} \right) \\ = & \mathbf{h} + \underbrace{\frac{1}{M} \left(\left\{ \mathbf{D}_{\mathrm{PF}}^{(\mathrm{P})} \right\}^{\mathrm{H}} \mathbf{D}_{\mathrm{PF}}^{(\mathrm{P})} \right)^{-1} \left\{ \mathbf{D}_{\mathrm{PF}}^{(\mathrm{P})} \right\}^{\mathrm{H}} \left(\overline{\mathbf{D}}_{\mathrm{DF}}^{(\mathrm{P})} \mathbf{h} + \frac{1}{R_{\mathrm{pd}}} \overline{\mathbf{w}}^{(\mathrm{P})} \right)}_{\mathbf{\Phi}} \end{aligned} \quad (8)$$

where $\overline{\mathbf{D}}_{\mathrm{DF}}^{(\mathrm{P})} = \sum_{\mathrm{m}=1}^{M} \left\{ \mathbf{D}_{\mathrm{DF}}^{(\mathrm{P})} \right\}_{\mathrm{m}}$, $\overline{\mathbf{w}}^{(\mathrm{P})} = \sum_{\mathrm{m}=1}^{M} \mathbf{w}_{\mathrm{m}}^{(\mathrm{P})}$ and $\mathbf{\Phi}$ is the channel estimation error vector whose size is $N_{\mathrm{t}} L \times 1$. The channel estimation error of the LS channel estimator σ_{LS}^2 [17] can be calculated in this case as

$$\begin{aligned} \sigma_{\mathrm{LS}}^2 &= \mathrm{E}\left[\mathrm{tr}\left[\mathbf{\Phi} \mathbf{\Phi}^{\mathrm{H}} \right] \right] = \mathrm{E}\{ ||\hat{\mathbf{h}} - \mathbf{h}||^2 \} \\ &= \sigma_{\mathrm{deg}}^2 \mathrm{tr}\left[\left(\left\{ \mathbf{D}_{\mathrm{PF}}^{(\mathrm{P})} \right\}^{\mathrm{H}} \mathbf{D}_{\mathrm{PF}}^{(\mathrm{P})} \right)^{-1} \right], \end{aligned} \quad (9)$$

where $\mathrm{tr}[\cdot]$ represents the trace of a matrix, and σ_{deg}^2 is the variance of the signal degradation which is composed of the data superimposed signal and the AWGN. If pilot symbols are equispaced and equipowered, thus

$$\sigma_{\mathrm{LS}}^2 = \sigma_{\mathrm{deg}}^2 \cdot \frac{L N_{\mathrm{t}}}{(1-\alpha)\mathcal{P}}. \quad (10)$$

The variance of the signal degradation σ_{deg}^2 can be written as

$$\sigma_{\mathrm{deg}}^2 = \frac{1}{M^2} \mathrm{E}\left[\overline{\mathbf{D}}_{\mathrm{DF}}^{(\mathrm{P})} \mathbf{h} \left\{ \overline{\mathbf{D}}_{\mathrm{DF}}^{(\mathrm{P})} \mathbf{h} \right\}^{\mathrm{H}} \right] + \frac{1}{R_{\mathrm{pd}}^2 M^2} \mathrm{E}\left[\overline{\mathbf{w}}^{(\mathrm{P})} \left\{ \overline{\mathbf{w}}^{(\mathrm{P})} \right\}^{\mathrm{H}} \right]. \quad (11)$$

In PSAM $\mathbf{D}_{\mathrm{DF}}^{(\mathrm{P})} = \mathbf{0}$, where $\mathbf{0}$ is an $N_{\mathrm{P}} \times L N_{\mathrm{t}}$ null matrix. By contrast, in ST the pilot and data sets are multiplexed in the same subcarriers, yielding a data interference represented by $\mathbf{D}_{\mathrm{DF}}^{(\mathrm{P})} \neq \mathbf{0}$. In ST, if M is large enough, the elements of $\overline{\mathbf{D}}_{\mathrm{DF}}^{(\mathrm{P})} = \sum_{\mathrm{m}=1}^{M} \left\{ \mathbf{D}_{\mathrm{DF}}^{(\mathrm{P})} \right\}_{\mathrm{m}}$ and $\overline{\mathbf{w}}^{(\mathrm{P})} = \sum_{\mathrm{m}=1}^{M} \mathbf{w}_{\mathrm{m}}^{(\mathrm{P})}$ can be modeled as a Gaussian distribution [18] with zero-mean and variance $M\mathcal{P}_{\mathrm{D}}/(N-2)$ and $M\sigma_{\mathrm{w}}^2$, respectively. It leads to represent the variance of the signal degradation at each technique as

$$\sigma_{\mathrm{deg,PSAM}}^2 = \frac{1}{R_{\mathrm{pd}}^2 M} \sigma_{\mathrm{w}}^2 \quad (12)$$

and

$$\sigma_{\mathrm{deg,ST}}^2 = \frac{\mathcal{P}_{\mathrm{D}}}{(N-2)M} \sigma_{\mathrm{H}}^2 + \frac{1}{R_{\mathrm{pd}}^2 M} \sigma_{\mathrm{w}}^2, \quad (13)$$

where $\sigma_{\mathrm{H}}^2 = \sum_{\mathrm{i}=1}^{N_{\mathrm{t}}} \sum_{l=0}^{L-1} h_{\mathrm{i}}^2(l) = \sum_{i=1}^{N_{\mathrm{t}}} \sigma_{\mathrm{H_i}}^2$ is the channel power.

B. Pilot sequences and pilot tones

The signal of superimposed pilots is composed of $N-2$ tones which can be generated in an optimal form. The minimum MSE when using ST or PSAM is achieved with an optimal pilot tone interval $N_{\mathrm{I}} = N/(N_{\mathrm{P}}/2)$ and an optimal pilot sequence [8]

$$[\mathbf{p}_{i\mathrm{half}}]_v = p_i(v) = e^{-j\frac{2\pi}{N_{\mathrm{P}}/2}\mu_i v}, v \in [1, N_{\mathrm{P}}/2], \quad (14)$$

creating

$$\mathbf{p}_i = \left[\mathbf{p}_{i\mathrm{half}} \quad \left\{ \mathbf{p}_{i\mathrm{half}}^{\mathrm{T}} \right\}^{\mathrm{H}} \right]^{\mathrm{T}}, \quad (15)$$

where $\mu_i \in \{0, 1, ..., N_{\mathrm{P}}/2 - 1\}$ is an integer value related to the i-th LED. Moreover, to guarantee orthogonality among pilots transmitted from different LEDs, the condition $\frac{\mu_{\mathrm{i}} - \mu_j + q - l}{N_{\mathrm{P}}/2} \notin \mathbb{Z}$ must be satisfied $\forall\, q, l \in \{1, ..., L\}$ and $i \neq j$, for example $\mu_i = (i-1)L + 1$.

Note that assuming perfect synchronization and given that orthogonal pilot sequences have been used for channel estimation, co-channel interference can be considered as negligible. The noise and interference produced will be even reduced by the averaging process applied over M OFDM symbols.

IV. Analysis of the spectral efficiency

Considering the total electrical transmit power $\mathrm{E}\left[\mathbf{x}^{\mathrm{H}}\mathbf{x}\right] = \mathcal{P}$ and the noise vector $\mathbf{w}$ whose elements follow a complex Gaussian distribution with variance σ_{w}^2, the signal-to-noise ratio (SNR) can be expressed as

$$\overline{\gamma} = \frac{R_{\mathrm{pd}}^2 \mathcal{P} \sum_{\mathrm{i}=1}^{N_{\mathrm{t}}} \sigma_{\mathrm{H_i}}^2}{(N-2) \cdot \sigma_{\mathrm{w}}^2}. \quad (16)$$

The received data symbols are represented by $\mathbf{y}_{\mathrm{PSAM}}^{(\mathrm{D})}$ and $\mathbf{y}_{\mathrm{ST}}^{(\mathrm{D})}$ in PSAM and ST cases, whose dimensions are $(N-2-N_{\mathrm{P}}) \times 1$ and $(N-2) \times 1$, respectively, corresponding to the elements of the subcarriers containing data symbols. In PSAM, these data symbols are directly extracted as

$$\begin{aligned} \mathbf{y}_{\mathrm{PSAM}}^{(\mathrm{D})} &= R_{\mathrm{pd}} \cdot \mathbf{D}_{\mathrm{DF}}^{(\mathrm{D})} \mathbf{h} + \mathbf{w}^{(\mathrm{D})} \\ &= R_{\mathrm{pd}} \cdot \mathbf{D}_{\mathrm{DF}}^{(\mathrm{D})} \left(\hat{\mathbf{h}} - \mathbf{\Phi} \right) + \mathbf{w}^{(\mathrm{D})}, \end{aligned} \quad (17)$$

where $\mathbf{D}_{\mathrm{DF}}^{(\mathrm{D})}$ and $\mathbf{w}^{(\mathrm{D})}$ are the $(N-N_{\mathrm{P}}-2) \times L N_{\mathrm{t}}$ matrix and $(N-N_{\mathrm{P}}-2) \times 1$ vector at the corresponding data positions, respectively. By contrast, in ST a subtraction of the pilots effect must be carried out as

$$\begin{aligned} \mathbf{y}_{\mathrm{ST}}^{(\mathrm{D})} &= R_{\mathrm{pd}} \cdot (\mathbf{D}_{\mathrm{DF}} + \mathbf{D}_{\mathrm{PF}}) \mathbf{h} - R_{\mathrm{pd}} \mathbf{D}_{\mathrm{PF}} \hat{\mathbf{h}} + \mathbf{w} \\ &= R_{\mathrm{pd}} \cdot \mathbf{D}_{\mathrm{DF}} \hat{\mathbf{h}} - R_{\mathrm{pd}} (\mathbf{D}_{\mathrm{DF}} + \mathbf{D}_{\mathrm{PF}}) \mathbf{\Phi} + \mathbf{w}. \end{aligned} \quad (18)$$

Note that the received data symbols in the ST case are affected by the pilot sequence because data and pilot symbols are multiplexed using all the available subcarriers. The signal-to-interference-plus-noise ratio (SINR) formulation at each case is written as

$$\overline{\gamma}_{\mathrm{PSAM}} = \frac{R_{\mathrm{pd}}^2 \frac{\mathcal{P}_{\mathrm{D}}}{N-N_{\mathrm{P}}-2} \cdot \sum_{\mathrm{i}=1}^{N_{\mathrm{t}}} \sigma_{\mathrm{H_i}}^2}{R_{\mathrm{pd}}^2 \cdot \sigma_{\mathrm{LS}}^2 \cdot \left(\frac{\mathcal{P}_{\mathrm{D}}}{N-N_{\mathrm{P}}-2} \right) + \sigma_{\mathrm{w}}^2}, \quad (19)$$

TABLE I: Optical system parameters

Parameter	Value	Unit
Room size	5x5x4	m
PD height	1	m
Detector area	1	cm^2
Semiangle at half optical power	60	deg.
Optical filter gain	1	-
Field of view at receiver	85	deg.
Refractive index of optical concentrator	1.5	-
PD responsivity, $R_{\rm pd}$	0.54	A/W
Individual reflectivities	0.8	-

and

$$\overline{\gamma}_{\rm ST}=\frac{R_{\rm pd}^2\frac{\mathcal{P}_{\rm D}}{N-2}\cdot\sum\limits_{\rm i=1}^{N_{\rm t}}\sigma_{\rm H_i}^2}{R_{\rm pd}^2\cdot\sigma_{\rm LS}^2\cdot\left(\frac{\mathcal{P}_{\rm D}}{N-2}+\frac{\mathcal{P}_{\rm P}}{N-2}\right)+\sigma_{\rm w}^2}. \quad (20)$$

Inserting the equations of data symbols and pilots power, the channel estimation error (10), the degradation signal (12) and (13) in (19) and (20) for PSAM and ST, respectively, the SINR at each case can be expressed as

$$\overline{\gamma}_{\rm PSAM}=\frac{(N-2)\cdot(1-\alpha)\cdot M}{\frac{1}{\overline{\gamma}}\left(L\cdot N_{\rm t}+M\cdot(N-2)\cdot(1-\alpha)\right)}, \quad (21)$$

and

$$\overline{\gamma}_{\rm ST}=\frac{\alpha\cdot(N-2)\cdot(1-\alpha)\cdot M}{L\cdot N_{\rm t}\cdot\left(\alpha+\frac{1}{\overline{\gamma}}\right)+(1-\alpha)\cdot M\cdot(N-2)\frac{1}{\overline{\gamma}}}. \quad (22)$$

After introducing a zero-mean Gaussian random variable with unitary variance g from the Shannon spectral efficiency definition [19], the spectral efficiency in the ideal case is calculated as

$$C_{\rm Ideal}=\frac{1}{N}\sum_{k=1}^{N/2-1}{\rm E}\left\{\log_2\left[1+\overline{\gamma}\cdot|g|^2\right]\right\}, \quad (23)$$

where all the available subcarriers for DCO-OFDM are used for transmitting data symbols at the maximum power $\mathcal{P}$ and the channel is assumed to be known. The lower bound for the spectral efficiency for PSAM and ST cases can be derived as

$$C_{\rm PSAM}=\frac{1}{N}\sum_{k\in\mathcal{K}_{\rm D}\cap\{1,\ldots,N/2-1\}}{\rm E}\left\{\log_2\left[1+\overline{\gamma}_{\rm PSAM}\cdot|g|^2\right]\right\}, \quad (24)$$

and

$$C_{\rm ST}=\frac{1}{N}\sum_{k=1}^{N/2-1}{\rm E}\left\{\log_2\left[1+\overline{\gamma}_{\rm ST}\cdot|g|^2\right]\right\}. \quad (25)$$

These metrics will be considered as spectral efficiency and compared to the ideal case ($C_{\rm Ideal}$).

In PSAM, a channel can be perfectly recovered in the absence of noise when pilots are equispaced and equipowered and $N_{\rm P}\geq N_{\rm t}L$. Since $N_{\rm P}$ in PSAM is computed as $N_{\rm P}=\lceil(1-\alpha)(N-2)\rceil$, where $\lceil\cdot\rceil$ represents rounding up to the next integer, for a given $N_{\rm t}$, L and N values, a maximum α value is determined as

$$\alpha_{\rm maxPSAM}=1-\frac{N_{\rm t}L}{N-2}. \quad (26)$$

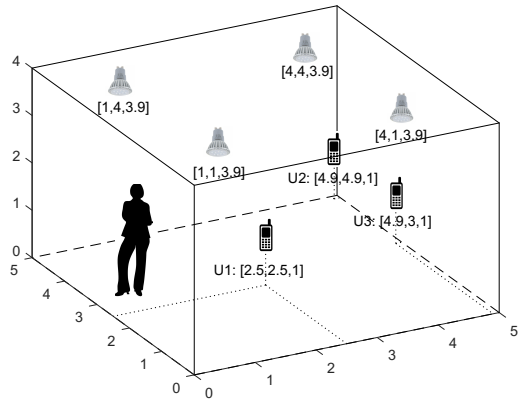

Fig. 1: VLC scenario. (The unit of coordinates is meter.)

For PSAM, an optimal value of α can be obtained as

$$\alpha_{\rm opt\,PSAM}=\underset{\alpha\in(0,\alpha_{\rm maxPSAM}]}{\arg\max}\ C_{\rm PSAM}(\alpha)=\max\left(0,\min(\alpha'_{\rm PSAM},\alpha_{\rm maxPSAM})\right), \quad (27)$$

where $\alpha'_{\rm PSAM}$ is computed through $\frac{\partial C_{\rm PSAM}}{\partial\alpha}=0$, yielding

$$\alpha'_{\rm PSAM}=\alpha:\log_2\left[1+\overline{\gamma}_{\rm PSAM}(\alpha)\right]=\frac{M(N-2)LN_{\rm t}}{\ln(2)\cdot\left(\frac{1}{\overline{\gamma}}\left(LN_{\rm t}+{\rm A}(\alpha)\right)+{\rm A}(\alpha)\right)\cdot\left(LN_{\rm t}+{\rm A}(\alpha)\right)} \quad (28)$$

where ${\rm A}(\alpha)=M(N-2)(1-\alpha)$.

In ST, all the available subcarriers transmit pilot symbols ($N_{\rm P}=N-2$) and, as a consequence, the parameter α can take values in all the range $0<\alpha<1$. An optimal value of α can be obtained analytically as

$$\alpha_{\rm opt\,ST}=\underset{\alpha\in(0,1)}{\arg\max}\ C_{\rm ST}(\alpha)=\max\left(0,\min(\alpha'_{\rm ST},1)\right), \quad (29)$$

where $\alpha'_{\rm ST}$ is computed through $\frac{\partial C_{\rm ST}}{\partial\alpha}=0$, yielding

$$\alpha'_{\rm ST}=\frac{M(N-2)+LN_{\rm t}-\sqrt{LN_{\rm t}\left(\overline{\gamma}+1\right)\left(LN_{\rm t}+M(N-2)\right)}}{M(N-2)-LN_{\rm t}\overline{\gamma}}. \quad (30)$$

Note that the larger the SNR $\overline{\gamma}$, the lower the $\alpha'_{\rm ST}$ is. It means that the power allocated to data symbols must be reduced to achieve the maximum spectral efficiency because, when the noise decreases, the interference produced by data symbols in ST is more significant compared to the noise. Finally, note that $\lim_{M\to\infty}\alpha'_{\rm ST}=1$, because the average of M OFDM symbols when M tends to ∞ eliminates the channel estimation error and then almost all the power should be assigned to data symbols in order to achieve the maximum spectral efficiency.

Note that any change in the CIR has a great influence in the spectral efficiency. This change can affect to the parameters M, L or $\overline{\gamma}$, representing the channel stationarity, the channel dispersion and the SNR dependent on the channel power as (16) shows, respectively.

V. Results

We consider a DCO-OFDM transmission system with $N=256$ subcarriers where the sampling rate evaluated is 500 MHz. The maximum tap delay is 30 ns resulting in L=16

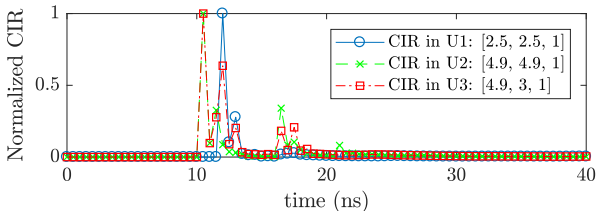

Fig. 2: CIR for three different user locations in the VLC scenario.

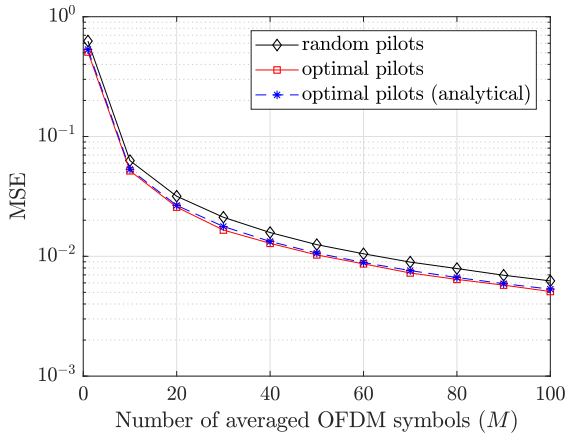

Fig. 3: Mean Squared Error of the ST scheme versus the number of averaged OFDM symbols, for a SNR $\overline{\gamma}$ = 10 dB, $\alpha = 0.8$.

taps following to a selection of a cyclic prefix (CP) equal to 16. The channel is generated by the ray tracing method [20] in a room whose characteristics and LED positions are described in Table I and represented in Fig. 1.

Fig. 2 represents the continuous CIR previous to be discretized in three different positions marked in Fig. 1 as U1, U2 and U3. As the user gets close to the walls, the reflections are stronger. Note that once the CIRs are discretized, the first tap is considered as the reference to the sampling period.

In Fig. 3 the MSE performance of the channel estimation is shown for a VLC scenario with SNR $\overline{\gamma} = 10$ dB and $\alpha = 0.8$. The theoretical expression deduced in (10) fits the performance obtained in the simulation results, which validates the theoretical study here presented. Note that the MSE becomes steady when M increases and the use of optimal pilots provides a better estimation. It is important to emphasize that the ST-VLC mechanism is applied under a scenario where the channel changes every M OFDM symbols which is known as quasi-stationary.

Table II shows the average CPU time against the number of OFDM symbols taken for the channel estimation in a MISO-ST-VLC system with two different pilots sequences: random and optimal pilots. The CPU time is calculated in Matlab 2017(a) using an Intel Core i5 4440 3.10GHz processor and running Microsoft Windows 7.

Fig. 4 represents the spectral efficiency as a function of the data power allocation factor α. An optimal α for each SNR value can be observed, which was theoretically derived in (27) and (29) for PSAM and ST, respectively, and they

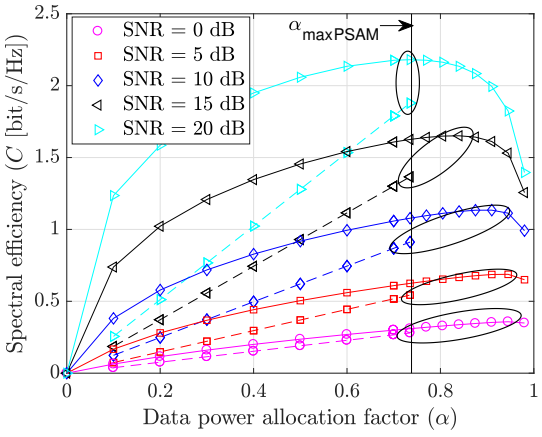

Fig. 4: Spectral efficiency (lower bound) versus α for ST (solid line) and PSAM (dashed line), for different SNR $\overline{\gamma}$ and $M = 200$.

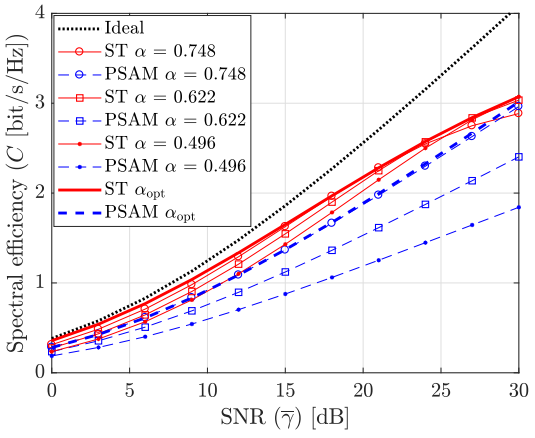

Fig. 5: Spectral efficiency of the ideal, ST and PSAM cases versus SNR for different values of α and $M = 200$.

closely match with simulation results. As expected, the higher the SNR, the better the spectral efficiency is. Besides, when α approaches 0 or 1, C_{ST} decreases because too much power is dedicated to either pilots or data, respectively. Superimposed training allows using α values in the whole range [0, 1], which permits to achieve larger values of spectral efficiency (see Fig. 4). It must be noted that for every SNR, the maximum spectral efficiency in ST is superior to the maximum spectral efficiency in PSAM, as highlighted with ellipses.

A comparison of ST and PSAM for different values of α as a function of SNR is shown in Fig. 5. ST outperforms PSAM at low and medium SNR values. In practical systems where from low to medium SNR values are faced, ST should be the preferred choice overcoming previous proposals as PSAM. We can see how the gradient of the spectral efficiency in ST alleviates at high SNR values because the noise decreases and the signal degradation only depends on the superimposed data signal. This behavior is typical in ST-based schemes. Since PSAM does not have superimposed data symbols over the pilot subcarriers, it does not suffer from such a degradation. In addition to the ideal curve showing the Shannon spectral

TABLE II: Average CPU time (s) of the MSE simulation

M	0	10	20	30	40	50	60	70	80	90	100
Random pilots	0.1299	0.1575	0.1877	0.2206	0.2515	0.2860	0.3136	0.3451	0.3752	0.4013	0.4394
Optimal pilots	0.1294	0.1564	0.1858	0.2178	0.2483	0.2814	0.3096	0.3395	0.3691	0.3951	0.4317

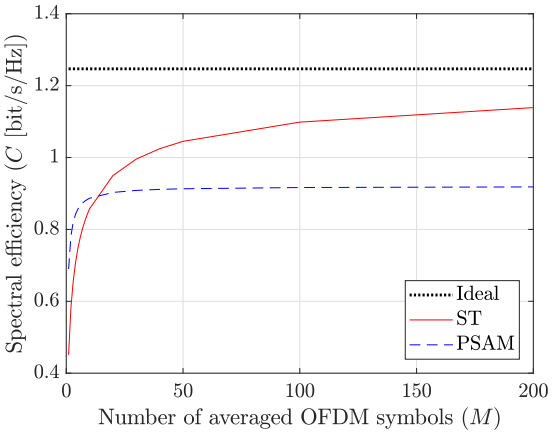

Fig. 6: Spectral efficiency of the ideal, ST and PSAM cases versus M for $\alpha{=}\alpha_{\text{opt}}$ and SNR $\overline{\gamma}{=}10$ dB.

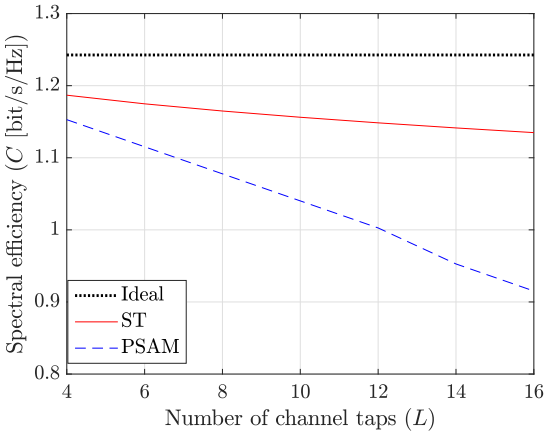

Fig. 7: Spectral efficiency of the ideal, ST and PSAM cases versus an increasing number of channel taps L for $\alpha{=}\alpha_{\text{opt}}$, $M{=}200$ and SNR $\overline{\gamma}{=}10$ dB.

efficiency, curves for ST and PSAM are plotted when an optimal value of α is employed. They demonstrate that we must use an optimal value of α for every value of SNR in order to maximize the spectral efficiency.

Fig. 6 illustrates the evolution of the spectral efficiency with respect to the increment of the channel stationarity represented by the number of OFDM symbols transmitted within the coherence time (M). The invoked α values are the optimal ones. Note that ST outperforms PSAM from low values of M where ST can correctly eliminate the interference due to the data symbols. Fig. 7 represents the spectral efficiency of ST and PSAM schemes versus the number of channel taps L for $\alpha{=}\alpha_{\text{opt}}$ and SNR $\overline{\gamma}{=}10$ dB. Note that the spectral efficiency decreases when the number of taps increases. That is, the more the channel dispersion, the worse the spectral efficiency is. However, the performance of ST deteriorates less than the one of PSAM. The reason is that superimposing all subcarriers allows the system to react better than PSAM to a highly dispersive channel.

VI. Conclusion

We have proposed a ST channel estimation method for a MISO DCO-OFDM VLC system. ST is an attractive strategy to increase the spectral efficiency mainly in scenarios where the channel exhibits a certain stationarity. Lower bounds of the spectral efficiency are derived when ST and PSAM are used. This analysis is valid for outdoor and indoor VLC scenarios. Additionally, the influence of the data power allocation factor, SNR and the number of averaged OFDM symbols is studied in such scenario. We conclude that ST outperforms PSAM in VLC from a certain M value on, and the variability in the dispersion of the channel affects to a lesser extent when using the ST technique.

References

[1] J. Wang, C. Jiang, H. Zhang, X. Zhang, V. C. M. Leung, and L. Hanzo, "Learning-aided network association for hybrid indoor LiFi-WiFi systems," *IEEE Trans. Veh. Technol.*, vol. 67, no. 4, pp. 3561–3574, Apr. 2018.

[2] Z. Wang, Q. Wang, W. Huang, and Z. Xu, *Visible Light Communications: Modulation and Signal Processing*. Wiley-IEEE Press, 2018.

[3] L. Zeng, D. C. O'Brien, H. L. Minh, G. E. Faulkner, K. Lee, D. Jung, Y. Oh, and E. T. Won, "High data rate multiple input multiple output (MIMO) optical wireless communications using white LED lighting," *IEEE J. Sel. Areas Commun.*, vol. 27, no. 9, pp. 1654–1662, Dec. 2009.

[4] Z. G. Sun, H. Y. Yu, W. C. Li, Z. J. Tian, and Y. J. Zhu, "Power-efficient linear precoding for MU-MISO VLC systems with channel uncertainty," *IEEE Photon. Technol. Lett.*, vol. 30, no. 7, pp. 626–629, Apr. 2018.

[5] Y. J. Zhu, Z. G. Sun, J. K. Zhang, Y. Y. Zhang, and J. Zhang, "Training receivers for repetition-coded MISO outdoor visible light communications," *IEEE Trans. Veh. Technol.*, vol. 66, no. 1, pp. 529–540, Jan. 2017.

[6] R. Mesleh, R. Mehmood, H. Elgala, and H. Haas, "Indoor MIMO optical wireless communication using spatial modulation," in *Proc. IEEE Int. Conf. Commun.*, Cape Town, South Africa, May 2010, pp. 1–5.

[7] Z. Yu, R. J. Baxley, and G. T. Zhou, "Multi-user MISO broadcasting for indoor visible light communication," in *Proc. IEEE Int. Conf. Acoust., Speech, Signal Process.*, Vancouver, Canada, May 2013, pp. 4849–4853.

[8] L. Wu, J. Cheng, Z. Zhang, J. Dang, and H. Liu, "Channel estimation for optical-OFDM-based multiuser MISO visible light communication," *IEEE Photon. Technol. Lett.*, vol. 29, no. 20, pp. 1727–1730, Oct. 2017.

[9] X. Chen and M. Jiang, "Adaptive statistical Bayesian MMSE channel estimation for visible light communication," *IEEE Trans. Signal Process.*, vol. 65, no. 5, pp. 1287–1299, Mar. 2017.

[10] J. K. Tugnait and S. He, "Multiuser/MIMO doubly selective fading channel estimation using superimposed training and Slepian sequences," *IEEE Trans. Veh. Technol.*, vol. 59, no. 3, pp. 1341–1354, Mar. 2010.

[11] X. Meng, J. K. Tugnait, and S. He, "Iterative joint channel estimation and data detection using superimposed training: algorithms and performance analysis," *IEEE Trans. Veh. Technol.*, vol. 56, no. 4, pp. 1873–1880, July 2007.

[12] J. C. Estrada-Jimenez, B. G. Guzman, M. J. F.-G. Garcia, and V. P. G. Jimenez, "Superimposed training-based channel estimation for visible light communications," in *Proc. Int. Wireless Commun. Mobile Comput. Conf.*, Valencia, Spain, June 2017, pp. 240–245.

[13] S. Dimitrov, S. Sinanovic, and H. Haas, "Clipping noise in OFDM-Based optical wireless communication systems," *IEEE Trans. Commun.*, vol. 60, no. 4, pp. 1072–1081, Apr. 2012.

[14] X. Ling, J. Wang, Z. Ding, C. Zhao, and X. Gao, "Efficient OFDMA for LiFi downlink," *J. Lightw. Technol*, vol. 36, no. 10, pp. 1928–1943, May 2018.

[15] C. Chen, D. A. Basnayaka, and H. Haas, "Downlink performance of optical attocell networks," *J. Lightw. Technol.*, vol. 34, no. 1, pp. 137–156, Jan. 2016.

[16] S. M. Kay, *Fundamentals of Statistical Signal Processing: Estimation Theory*, 1993.

[17] I. Barhumi, G. Leus, and M. Moonen, "Optimal training design for MIMO OFDM systems in mobile wireless channels," *IEEE Trans. Signal Process.*, vol. 51, no. 6, pp. 1615–1624, June 2003.

[18] W. C. Huang, C. P. Li, and H. J. Li, "On the power allocation and system capacity of OFDM systems using superimposed training schemes," *IEEE Trans. Veh. Technol.*, vol. 58, no. 4, pp. 1731–1740, May 2009.

[19] M. Medard, "The effect upon channel capacity in wireless communications of perfect and imperfect knowledge of the channel," *IEEE Trans. Inf. Theory*, vol. 46, no. 3, pp. 933–946, May 2000.

[20] J. R. Barry, J. M. Kahn, W. J. Krause, E. A. Lee, and D. G. Messerschmitt, "Simulation of multipath impulse response for indoor wireless optical channels," *IEEE J. Sel. Areas Commun.*, vol. 11, no. 3, pp. 367–379, Apr. 1993.